PHYSICAL REVIEW A VOLUME 40, NUMBER 5 SEPTEMBER 1, 1989

Semiclassical theory of a micromaser

A. M. Guzman,* P. Meystre, and E. M. Wright
Optical Sciences Center, University of Arizona, Tucson, Arizona 85721
(Received 4 May 1989)

We present a semiclassical theory of the micromaser by using a consistent multiple-time-scale expansion of its dynamics. The time scale over which the semiclassical approximation is valid is established, and the effects of quantum and thermal fluctuations in the long-time limit are investigated. A thermodynamical analogy is introduced to interpret the steady-state properties of the micromaser, and we show that a simple model allowing for two-phase coexistence provides the best agreement between the semiclassical and quantum theories.

I. INTRODUCTION

The emerging field of cavity QED (quantum electrodynamics) makes possible experiments that probe the fine details of the interaction between the radiation field and one or a few atoms.[1] In particular, by using extremely high-Q microwave cavities experiments can be performed in which a single mode of the radiation is essentially isolated from its environment allowing the observation of genuine quantum features which are normally masked by environmental fluctuations. This is the case in micromasers[2,3] in which a monoenergetic beam of excited Rydberg atoms is injected at such a low rate that at most one atom at a time is present in the cavity. In such systems the combined effects of the high-Q cavity and the large dipole moment of the Rydberg atoms means that the maser threshold can be reached even for such low injection rates. Both one-photon[2] and two-photon[3] micromasers have been theoretically analyzed[4,5] and have been shown to exhibit a number of unique characteristics that are "washed out" by classical and quantum fluctuations in conventional laser and maser systems.

One of the attractive properties of systems such as micromasers is that they provide a means to experimentally investigate the transition between truly microscopic and macroscopic systems. From this point of view, they might help shed light on the quantum-classical correspondence in systems directly amenable to experimental verification.

This paper presents a semiclassical theory of the micromaser based on a consistent multiple-time-scale expansion of its dynamics. This approach allows one to distinguish a short-time evolution, which is essentially semiclassical, from the long-time evolution where noise and quantum diffusion play essential roles. Furthermore, using this approach, it becomes obvious that the steady-state and semiclassical limits do not commute. Hence the steady-state properties of the micromaser exhibit characteristics that can be related immediately to quantum (as well as thermal) fluctuations. Indeed, we show that provided subtle effects such as low-temperature trapping[6] and quantum revivals[7] can be ignored the steady-state properties of the micromaser can be understood as resulting from an equal-area Maxwell construction between multistable semiclassical steady states. Because the time scale over which this noise-induced equilibration takes place can be varied almost at will, the micromaser offers a unique experimental situation to study such transitions between classical and quantum behavior.

The rest of this paper is organized as follows. Section II briefly reviews the quantum theory of the micromaser in order to define the model and introduce our notation. In Sec. III we derive a Fokker-Planck equation for the photon statistics, employing the classical Becker-Döring theory.[8] Section IV then develops a semiclassical theory of the micromaser based on the Fokker-Planck equation (3.8). Normally one obtains the underlying deterministic theory by considering the drift term alone. Our analysis is based on a multiple-time-scale analysis which sheds some light on the nature of the semiclassical theory, and, in particular, shows explicitly why the steady-state and semiclassical limits do not commute. A thermodynamic analogy shows how the quantum steady-state properties of the micromaser can be understood in terms of a Maxwell construction over the multistable semiclassical solutions. Finally, Sec. V is a summary and conclusion.

II. QUANTUM THEORY OF THE MICROMASER

We consider a micromaser system consisting of a high-Q single-mode cavity into which excited two-level atoms are injected at such a low rate that there is at most one atom present in the cavity at any given time.[2] The atomic beam is taken to be monoenergetic, each atom spending a time $t_{\rm int}$ in the cavity which has a damping time γ^{-1}. The successive atoms enter the cavity according to a Poisson distribution with mean rate R, $1/R$ being the mean time between atoms. We further assume that $t_{\rm int} \ll \gamma^{-1}$, so that damping may be ignored while an atom is in the cavity. Under these conditions, the statistically averaged density operator for the field obeys the master equation[4]

$$\frac{\partial \rho_f}{\partial t} = L\rho_f + R\,[F(t_{\rm int}) - I]\rho_f \ . \tag{2.1}$$

The Liouvillian L accounts for damping of the cavity

mode as given by the standard master equation for a damped harmonic oscillator,[9]

$$L\rho_f=(\gamma/2)(n_b+1)(2a\rho_f a^\dagger-a^\dagger a\rho_f-\rho_f a^\dagger a)$$
$$+(\gamma/2)n_b(2a^\dagger\rho_f a-aa^\dagger\rho_f-\rho_f aa^\dagger)\ , \quad (2.2)$$

n_b being the mean number of thermal photons in the bath. The atom-field interaction is described by

$$F(t_{\rm int})\rho_f(t)\equiv{\rm Tr}_a[U(t_{\rm int})\rho(t)U^\dagger(t_{\rm int})]\ . \quad (2.3)$$

Here, $\rho(t)$ is the combined atom-field density operator at time t, $U(t_{\rm int})=\exp(-iHt_{\rm int}/\hbar)$ is the evolution operator for the Jaynes-Cummings Hamiltonian H describing the dipole interaction between the cavity mode and a two-level atom, and ${\rm Tr}_a$ denotes the trace over the atomic variables. For exact resonance between the cavity mode and atomic transition frequencies ω, the Jaynes-Cummings Hamiltonian is[10]

$$H\equiv(\hbar\omega/2)S_3+\hbar\omega a^\dagger a+(\hbar\kappa/2)(S_+a+a^\dagger S_-)\ , \quad (2.4)$$

where S_3, S_+, and S_- are the atomic spin operators, a and $a^\dagger$ are the usual boson operators obeying $[a,a^\dagger]=1$, and κ is the atomic dipole moment.

It is sufficient for our purposes to assume that the field density matrix is initially diagonal in the number state representation (e.g., a thermal field), and that the atoms are injected in their upper state. It can then be shown that the field density matrix remains diagonal for all times during the evolution described by Eq. (2.1). We concentrate on these diagonal elements, which define the photon statistics

$$p_n(t)=\langle n|\rho_f(t)|n\rangle\ . \quad (2.5)$$

The time evolution of $p_n(t)$ is given by the master equation[4]

$$\frac{\partial p_n}{\partial t}=\gamma(n_b+1)[(n+1)p_{n+1}-np_n]$$
$$+\gamma n_b[np_{n-1}-(n+1)p_n]$$
$$+\gamma N_{\rm ex}(\beta_n p_{n-1}-\beta_{n+1}p_n)\ . \quad (2.6)$$

Here, $N_{\rm ex}=R/\gamma$ is the mean number of atoms which traverse the cavity during a field lifetime γ^{-1} and

$$\beta_n=\sin^2[\Theta(n/N_{\rm ex})^{1/2}]\ . \quad (2.7)$$

The parameter $\Theta=\kappa t_{\rm int}(N_{\rm ex}^{1/2})/2$ plays the role of a pump parameter, the micromaser threshold occurring at $\Theta\cong 1$.

Equation (2.6) is the starting point for our discussion of the semiclassical theory of the micromaser. Its steady-state solution is

$$p_n=C\left[\frac{n_b}{1+n_b}\right]^n\prod_{k=1}^{n}\left[1+\frac{N_{\rm ex}}{n_b}\frac{\beta_k}{k}\right]\ , \quad (2.8)$$

where C is a normalization constant. The features of the steady-state photon statistics are discussed in Ref. 4, along with the behavior of the average photon number

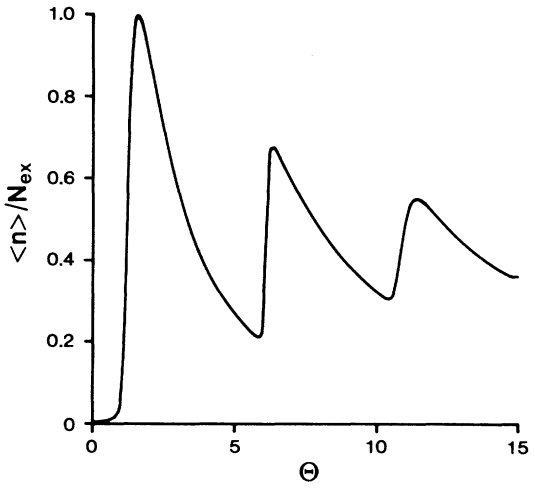

FIG. 1. Normalized mean photon number $\langle n\rangle/N_{\rm ex}$ as a function of the pump parameter Θ for $N_{\rm ex}=200$, and $n_b=1$. The first maser threshold occurs at $\Theta\cong 1$, and the higher-order thresholds appear at $\Theta\cong 2k\pi$, k an integer.

$$\langle n\rangle=\sum_{k=0}^{\infty}kp_k\ . \quad (2.9)$$

The onset of maser oscillations is followed by a succession of abrupt transitions in the state of the field. This is illustrated in Fig. 1, where we show $\langle n\rangle/N_{\rm ex}$ as a function of Θ for $N_{\rm ex}=200$, and $n_b=1$. For smaller values of $N_{\rm ex}$ the higher maser thresholds become less pronounced. The sharpness of the thresholds suggests that in the limit $N_{\rm ex}\to\infty$ the first (maser) threshold may be interpreted as a second-order phase transition, whereas the others are similar to first-order phase transitions.[4]

III. FOKKER-PLANCK APPROACH

A. Fokker-Planck equation

In Sec. IV we use a multiple-time-scale analysis to isolate three fundamental time scales of interest in the dynamics of the micromaser. The semiclassical approximation is introduced in terms of these time scales, which have a simple interpretation in terms of an effective potential. This effective potential is, in turn, best understood in terms of a Fokker-Planck equation describing the dynamics of the micromaser photon statistics. In the present section we derive this Fokker-Planck equation using the classical Becker-Döring theory as described in Ref. 8.

We proceed by noting that the master equation (2.6), which determines the probability p_n of finding n photons in the cavity mode at time t, can be written in the form

$$\frac{\partial p_n}{\partial t}=J_{n-1}-J_n,\quad n\geq 1\ . \quad (3.1)$$

Here, J_n is the net probability current between states with photon number n and $n+1$, and is given by

$$J_n=\mathscr{g}_n p_n-l_{n+1}p_{n+1}\ , \quad (3.2)$$

$\mathscr{g}_n$ is a gain rate and l_n a loss rate. Figure 2 illustrates how the photon statistics may change due to these rates. Explicit expressions for $\mathscr{g}_n$ and l_n are easily found by comparison with Eq. (2.6),

$$\mathscr{g}_n=\gamma N_{\rm ex}\beta_{n+1}+\gamma n_b(n+1)\ , \tag{3.3a}$$

$$l_n=\gamma(1+n_b)n\ . \tag{3.3b}$$

Note that since the atoms are injected in their excited state, the field-atom–interaction probability current always flows from lower to higher photon number states.

The steady-state photon statistics can be obtained from Eq. (3.1) by setting $\partial p_n/\partial t$ to zero: this gives the recursion relation $J_n=J_{n-1}$ for the probability currents, which implies $J_n=0$ for all n if the probability current is required to be zero as n goes to infinity. In this way the steady-state photon statistics (2.8) are recovered.

A continuous Fokker-Planck can be obtained by neglecting the discrete nature of n, replacing the difference terms of the master equation (3.1) by differentials, and representing p_n, l_n, and $\mathscr{g}_n$ by functions $p(n)$, $l(n)$, and $\mathscr{g}(n)$ of the now continuous variable n. Terms like $l(n+1)p(n+1,t)$ on the right-hand side of (3.1) are expanded in terms of $p(n,t)$ and $l(n)$ according to

$$l(n+1)p(n+1,t)=\sum_{k=0}\left[\frac{1}{k!}\frac{\partial^k}{\partial n^k}\right]l(n)p(n,t)\ . \tag{3.4}$$

We obtain a Fokker-Planck equation by truncating all such expansions at second order. Although the expansion (3.4) is formally exact as k goes to infinity, the validity of the truncation is questionable. However, the Pawula theorem tells us that the truncation either stops at second order, or an infinite number of terms are required.[11] We shall return to the validity of the Fokker-Planck equation below, but for the moment we simply proceed by truncating the expansions to get

$$\frac{\partial p(n,t)}{\partial t}=-\frac{\partial}{\partial n}[Q(n)p(n,t)]+\frac{1}{2}\frac{\partial^2}{\partial n^2}[G(n)p(n,t)]\ , \tag{3.5}$$

where

$$Q(n)=\mathscr{g}(n)-l(n)=\gamma n_b-\gamma n+\gamma N_{\rm ex}\beta_{n+1} \tag{3.6a}$$

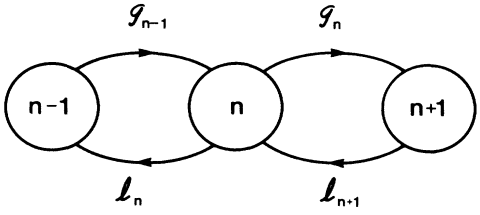

FIG. 2. Schematic representation of the flow of probability due to the gain and loss rates $\mathscr{g}_n$ and l_n.

and

$$G(n)=\mathscr{g}(n)+l(n)=\gamma n+2\gamma n_b n+\gamma n_b+\gamma N_{\rm ex}\beta_{n+1}\ . \tag{3.6b}$$

The same Fokker-Planck equation was obtained in Ref. 4 by evaluating the moments for the change in photon number as a definite number of atoms traverse the cavity. The diffusion coefficient $G(n)$ contains not only stochastic fluctuations proportional to γ due to the coupling of the system to a thermal bath, but also a quantum-noise term proportional to $\gamma N_{\rm ex}=R$ resulting from the quantized atom-field interaction.

For calculational purposes it proves useful to introduce the scaled quantities

$$\tau=\gamma t,\quad \nu=n/N_{\rm ex},\quad P(\nu,t)=N_{\rm ex}p(\nu,t)\ , \tag{3.7}$$

in terms of which the Fokker-Planck equation becomes

$$\frac{\partial P(\nu,\tau)}{\partial\tau}=-\frac{\partial}{\partial\nu}[q(\nu)P(\nu,\tau)]+\frac{1}{2N_{\rm ex}}\frac{\partial^2}{\partial\nu^2}[g(\nu)P(\nu,\tau)]\ , \tag{3.8}$$

where

$$q(\nu)=n_b/N_{\rm ex}-\nu+\sin^2[\Theta(\nu+1/N_{\rm ex})^{1/2}] \tag{3.9a}$$

and

$$g(\nu)=\nu+2n_b\nu+n_b/N_{\rm ex}+\sin^2[\Theta(\nu+1/N_{\rm ex})^{1/2}]\ . \tag{3.9b}$$

It is easy to verify that the normalization of the photon number distribution $P(\nu,\tau)$ is

$$\int_0^\infty d\nu\,P(\nu,\tau)=1\ . \tag{3.10}$$

The moments of the photon distribution can be calculated from $P(\nu,\tau)$. For example, the continuous version of Eq. (2.9) is

$$\langle\nu\rangle=\int_0^\infty d\nu\,\nu P(\nu,\tau)\ . \tag{3.11}$$

To conclude this section, we remark that, although we have used the classical Becker-Dörring theory to obtain the Fokker-Planck equation, the resulting theory is still intrinsically quantum mechanical. By restricting our interest to the diagonal elements of the field density matrix, we are dealing with classical-like probabilities which describe the occupation of the photon number states. However, the gain and loss rates given by Eqs. (3.3) are obtained from quantum theory and the resulting theory is therefore quantum mechanical.

B. Steady-state solution

The steady-state solution of the Fokker-Planck equation (3.8) is easily obtained by assuming natural boundary conditions, which are required to give a normalizable solution. By setting $\partial P/\partial\tau=0$ and integrating Eq. (3.8) we obtain

$$P(\nu)=P(0)\left[\frac{g(0)}{g(\nu)}\right]\exp[-2N_{\rm ex}V(\nu)]\ , \tag{3.12a}$$

where the "effective potential" $V(\nu)$ is given by

$$V(\nu)=-\int_0^{\nu}\frac{d\nu' q(\nu')}{g(\nu')}\ . \tag{3.12b}$$

Notice that, from Eq. (3.9b), $g(\nu)$ is nonzero and positive on the whole range $(0,\infty)$, so that $P(\nu)$ is positive definite and normalizable. The extrema of $V(\nu)$ are found by requiring that $\partial V/\partial\nu=0$, or $q(\nu)=0$. We label these minima by $\nu=\nu_m$, $m=1,2,\ldots$.

Most of our considerations in the rest of this paper concern the limit $N_{\rm ex}\gg 1$. In that limit, the exponential term in (3.12a) will dominate the behavior of the maser. In particular, it is clear that the photon-number distribution $P(\nu)$ will tend to accumulate in the global minimum of the effective potential $V(\nu)$.

C. Range of validity

We now return to the question of the range of validity of the continuous Fokker-Planck approximation. The obvious requirement is that $\nu=n/N_{\rm ex}$ should represent a quasicontinuous variable. Since n is a discrete variable taking on integer values only, we have $d\nu=1/N_{\rm ex}$. Therefore, the Fokker-Planck equation is only strictly valid in the limit

$$N_{\rm ex}\gg 1\ . \tag{3.13}$$

The second requirement concerns the derivation of the Fokker-Planck equation, in which $p(n+1)$ is represented in terms of $p(n)$ and its derivatives. This approximation is equivalent to considering the expansion

$$P(\nu+1/N_{\rm ex})=P(\nu)+\frac{1}{N_{\rm ex}}\frac{\partial P(\nu)}{\partial\nu}+\cdots\ , \tag{3.14}$$

in terms of the scaled quantities. For the expansion to truncate, we require that the first-order correction is much smaller than $P(\nu)$, or

$$\left|\frac{1}{P}\frac{\partial P}{\partial\nu}\right|\ll N_{\rm ex}\ . \tag{3.15}$$

Another expression for the left-hand side of Eq. (3.15) can be obtained from Eqs. (3.12): We assume that $N_{\rm ex}\gg 1$, so that the exponential term dominates the behavior of $P(\nu)$. Then by differentiating (3.12a) with respect to ν, we obtain

$$\left|\frac{1}{P}\frac{\partial P}{\partial\nu}\right|\cong 2N_{\rm ex}|q(\nu)|/g(\nu)\ . \tag{3.16}$$

We now use Eqs. (3.9) for $q(\nu)$ and $g(\nu)$, and consider the limits $1/N_{\rm ex}\to 0$, $n_b/N_{\rm ex}\to 0$, to obtain, from Eqs. (3.15) and (3.16),

$$\nu+2n_b\nu+\sin^2(\Theta\sqrt{\nu})\gg 2|\nu-\sin^2(\Theta\sqrt{\nu})|\ . \tag{3.17}$$

In the worst case the left-hand side should be made as small as possible and the right-hand side as large as possible for a given ν. We therefore set the sin term equal to zero, from which we obtain

$$n_b\gg\tfrac{1}{2}\ . \tag{3.18}$$

Hence the Fokker-Planck equation is only valid at sufficiently large values of the thermal photon number.

These limitations to the range of validity of the Fokker-Planck equation can be understood as follows. The parameter $N_{\rm ex}$ is the mean number of atoms that traverse the cavity in a field lifetime. Above the first maser threshold the mean number of photons in the cavity is roughly $N_{\rm ex}$, due to the balancing of atomic pumping and field decay. Therefore, a large value of $N_{\rm ex}$ generally means a large value of the mean photon number. In this regime the gain and loss rates given by Eqs. (3.3) become relatively insensitive to replacing n by $n+1$ for $n\cong N_{\rm ex}\gg 1$, which is certainly required for the Fokker-Planck approximation to hold. However, we also require that the photon statistics p_n vary slowly with n. In this regard the presence of thermal photons tends to smoothen the photon statistics p_n since cavity dissipation leads to the transfer of probability both upward $(n\to n+1)$ and downward $(n+1\to n)$, as seen from the master equation (2.6). Therefore, for n_b large enough, it becomes impossible for the photon statistics to become sharply peaked. Thus, for high enough thermal photon numbers and $N_{\rm ex}\gg 1$, the photon statistics may be treated as smooth and quasicontinuous, and the Fokker-Planck equation is valid. We note that this is also the range of parameters for which effects such as collapse and revival[7] in the mean photon number do not occur. Note also that for $n_b\to 0$ only downward transitions are allowed by the master equation (2.6). This leads to micromaser dynamics dominated by the existence of "trapping states," as discussed in Ref. 6. Such effects rely upon the discrete nature of the radiation-field photon statistics, and are beyond the scope of the Fokker-Planck approximation.

Numerical calculations show that the range of validity of the Fokker-Planck approximation is not as stringent as indicated by Eqs. (3.13) and (3.18). We have found that the Fokker-Planck equation provides accurate results for n_b as low as 1, and $N_{\rm ex}$ as low as 20. This is illustrated in the numerical examples presented in later sections.

IV. SEMICLASSICAL THEORY

A. Semiclassical rate equation

In this section we develop a semiclassical theory of the micromaser based on the Fokker-Planck equation (3.8). Normally one obtains the underlying deterministic theory by considering the drift term $q(\nu)$ alone. [In the presence of multiplicative noise one also has noise-induced drift arising from $g(\nu)$.] Rather than following this path, we give an analysis based on a multiple-time-scale analysis, which sheds some light on the nature of the semiclassical theory.

Filipowicz *et al.*[4] and Davidovich *et al.*[5] have previously discussed the approach to equilibrium in micromasers. They identified two main time scales, namely τ_l,

which governs the redistribution of the photon-number distribution around a local minimum ν_m (not necessarily the global minimum) of the effective potential $V(\nu)$, and a second one, τ_g, which gives the passage time of the system towards the global minimum of the effective potential. The passage time behaves qualitatively like $\tau_g \cong \exp(\alpha N_{\rm ex})$, where $\alpha > 0$ is of order unity, and is therefore very large in the limit $N_{\rm ex} \gg 1$. In contrast, the approach to quasiequilibrium inside a local minimum occurs on a time scale $\tau_l \cong 1$. Filipowicz *et al.* obtained a Gaussian approximation,[4]

$$P(\nu) = \frac{1}{\sqrt{2\pi}\sigma} \exp[-(\nu-\nu_m)^2/2\sigma^2] , \tag{4.1a}$$

to the quasiequilibrium solution $P(\nu)$ around ν_m, where the rms spread σ is given by

$$\sigma^2 = g(\nu_m)/2N_{\rm ex}|q'(\nu_m)| . \tag{4.1b}$$

In general, $g(\nu_m) \cong |q'(\nu_m)| \cong 1$, and it follows that $\sigma \cong N_{\rm ex}^{-1/2}$. In general terms, the message from these results is very clear: any initial photon-number distribution evolves towards a distribution with dispersion σ on a relatively short time scale τ_l. In the case $N_{\rm ex} \gg 1$, σ can be made arbitrarily small, in which case $P(\nu,t)$ represents a well-defined number of photons. This notion is central to the semiclassical theory of the micromaser.

To proceed with our analysis, we return to Eq. (3.8) and introduce the successive time scales $\tau_m = \epsilon^m \tau$, where $\epsilon = 1/N_{\rm ex} \ll 1$. Here, τ_0 is the fastest or fundamental time scale, τ_1 is the lowest-order slow time scale, and so on for $m > 1$. In the usual manner, the τ_m are then taken as independent variables, with

$$\frac{\partial}{\partial\tau} = \frac{\partial}{\partial\tau_0} + \epsilon\frac{\partial}{\partial\tau_1} + \epsilon^2\frac{\partial}{\partial\tau_2} + \cdots . \tag{4.2a}$$

We accordingly expand $P(\nu,\tau)$ as

$$P(\nu,\tau) = \sum_{m=0}^{\infty} \epsilon^m P^{(m)}(\nu,\tau_0,\tau_1,\ldots) . \tag{4.2b}$$

By substituting Eqs. (4.2) into (3.8), we obtain a hierarchy of equations for the $P^{(m)}$ by comparing terms in powers of ϵ. To lowest order, ϵ^0, we obtain

$$\frac{\partial P^{(0)}(\nu,\tau_0)}{\partial\tau_0} = -\frac{\partial}{\partial\nu}[q(\nu)P^{(0)}(\nu,\tau_0)] . \tag{4.3}$$

To this order there is no diffusion effect as described by $g(\nu)$. Equation (4.3) is valid for times τ less than the characteristic slow time scale, which we denote by $\tau_{\rm sc} \cong N_{\rm ex}$.

Under the restriction that we are considering times $\tau < \tau_{\rm sc}$, we can now use Eq. (4.3) to obtain a semiclassical theory. For simplicity in notation we replace $\tau_0 \to \tau$, $P^{(0)} \to P$. We consider a solution of (4.3) of the form

$$P(\nu,\tau) = \delta_\sigma(\nu - \langle\nu(\tau)\rangle) . \tag{4.4}$$

Here the subscript σ indicates that we are using a representation of the delta function with dispersion σ which becomes exact as $\sigma \to 0$, e.g., Eq. (4.1a). We assume that $N_{\rm ex}$ is large enough (σ small enough) that $\delta_\sigma(x)$ behaves in all respects like $\delta(x)$ for our calculations. This notion is required since we know that, if we start from a photon-number distribution $P(\nu,0) = \delta(\nu - \langle\nu(0)\rangle)$, which has zero dispersion, then for $\tau \geq 1$ the distribution will become of the form (4.4). In this way our analysis acknowledges the time scale τ_l.

We proceed by substituting Eq. (4.4) into (4.3) to obtain the semiclassical rate equation

$$\begin{aligned}\frac{d\langle\nu\rangle}{d\tau} &= q(\langle\nu\rangle) \\ &= -(\langle\nu\rangle - n_b/N_{\rm ex}) \\ &\quad + \sin^2[\Theta(\langle\nu\rangle + 1/N_{\rm ex})^{1/2}] .\end{aligned} \tag{4.5}$$

This same equation was also obtained by Filipowicz *et al.*,[4] although they did not discuss its range of validity. From the preceding discussion it is clear that, in dimensional units, $t_{\rm sc} \cong N_{\rm ex}\gamma^{-1}$ is the time scale on which the semiclassical rate equation is valid.

In these same dimensional units Eq. (4.5) becomes

$$\begin{aligned}\frac{d\langle n\rangle}{dt} &= -\gamma(\langle n\rangle - n_b) \\ &\quad + R\sin^2\{\Theta[(\langle n\rangle + 1)/N_{\rm ex}]^{1/2}\} .\end{aligned} \tag{4.6}$$

We have compared the results from Eq. (4.5) with those from the full quantum theory and have found reasonable agreement between the two within the range of validity of the theory and for short enough times. The results of these dynamical calculations will be the subject of a future publication. In this paper we concentrate on the steady-state solution of Eq. (4.5), with $d\langle\nu\rangle/dt = 0$. From Eq. (4.5), it is clear that the steady-state solutions obey $q(\langle\nu\rangle) = 0$, which, in turn, correspond to the extrema of the effective potential V in Eq. (3.12b). They can be found graphically by solving (4.5) for Θ as a function of $\langle\nu\rangle$:

$$\Theta = \frac{\arcsin(\langle\nu\rangle - n_b/N_{\rm ex})}{(\langle\nu\rangle + 1/N_{\rm ex})^{1/2}} . \tag{4.7}$$

Figure 3 shows the steady-state normalized "mean photon number" $\langle\nu\rangle$ versus Θ for $n_b = 1$, $N_{\rm ex} = 100$. Several features are immediately apparent. For $\Theta \leq 5$ the curve is very similar to that obtained from quantum mechanics, showing, in particular, the sharp first maser threshold, but for $\Theta \geq 5$ large deviations are obvious. In particular, it is seen that $\langle\nu\rangle$ becomes a multivalued function of Θ. This is in sharp contrast to the quantum-mechanical result, where $\langle n\rangle/N_{\rm ex}$ is uniquely determined by Θ; see, e.g., Fig. 1. (Note that $\langle\nu\rangle$ corresponds directly to the quantity $\langle n\rangle/N_{\rm ex}$ in the quantum theory.) The dotted portion of the curve indicates those solutions which are unstable according to the semiclassical equation (4.5). The stability is determined in the usual way by linearizing around the steady-state solution and checking the growth rate of perturbations. In this semiclassical picture the micromaser displays the classic characteristics of a multistable system in which the negative-slope regions of the "input-output" curve are unstable.

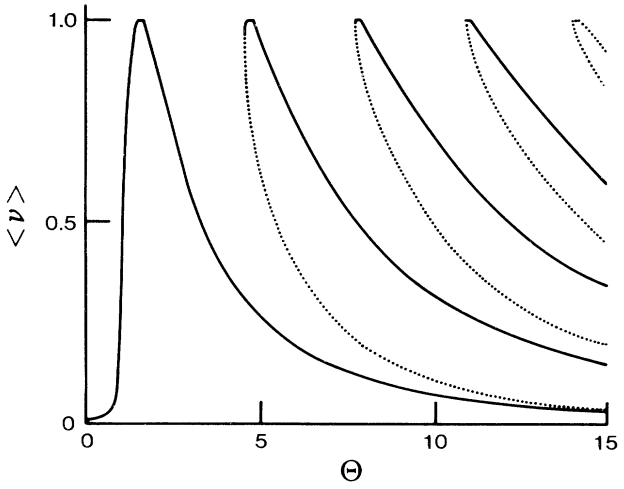

FIG. 3. Semiclassical mean photon number $\langle n \rangle$ vs Θ for $N_{ex}=100$, and $n_b=1$. The dotted line indicates the unstable branches according to the semiclassical rate equation (4.5).

Figure 4 shows a comparison of the semiclassical steady states and the corresponding quantum-mechanical calculation. The quantum result shows a series of higher-order thresholds characterized by a transition from one branch of the semiclassical solution to the next highest. Our semiclassical theory cannot, however, provide any indication of when these transitions occur.

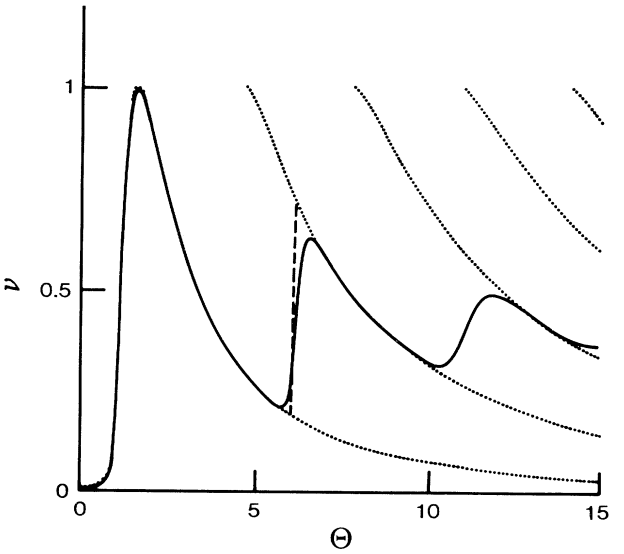

FIG. 4. Comparison of quantum and semiclassical steady-state results for the mean photon number as a function of Θ, for $N_{ex}=100$, and $n_b=1$. The solid line is the result from the full quantum calculation, and the dotted lines are the stable branches according to the Fokker-Planck approach. The vertical dashed lines shows the transition between the first and second branches predicted by Eq. (4.10b).

B. Quantum diffusion

The reason for the inadequacy of the semiclassical rate equation to properly reproduce the steady-state quantum results is that to describe the steady-state one must consider the limit $\tau \to \infty$. This implies that Eq. (4.5) is inadequate since it is restricted to $\tau < \tau_{sc}$. For $\tau > \tau_{sc}$, higher-order corrections $P^{(m)}$ must be kept in Eq. (4.2b). It is straightforward to show that all these higher-order terms depend on the diffusion term $g(n)$ in the Fokker-Planck equation. Physically, the appearance of the diffusion term for large times leads to broadening and redistribution of the initial photon-number distribution. We have seen that in the regime of the semiclassical approximation the photon-number distribution (4.4) is sharply peaked with dispersion $\sigma \cong N_{ex}^{-1/2}$. In contrast, times $\tau > \tau_{sc}$ are characterized by the onset of quantum diffusion, which causes the passage of the system towards the global minimum of the effective potential. The photon-number distribution reshapes and may become multipeaked. Alternatively, one may view Eq. (4.5) as the lowest-order approximation to a stochastic differential equation in which the fluctuating noise source may be neglected for $\tau < \tau_{sc}$. This interpretation relies on the fact that, in the distribution sense, the Fokker-Planck equation is equivalent to a stochastic differential equation, the noise being related to the diffusion coefficient $g(n)$. From either point of view, in the asymptotic limit $\tau \to \infty$ the photon statistics must always evolve to the solution given by Eq. (3.12), so that in steady-state quantum (and thermal) diffusion effects are always present.

To understand the role of quantum diffusion, we return to Eqs. (3.12) for the steady-state photon-number distribution, which we reproduce here for clarity in presentation,

$$P(n)=P(0)\left[\frac{g(0)}{g(n)}\right]\exp[-2N_{ex}V(n)] , \tag{4.8}$$

$$V(n)=-\int_0^n \frac{dn'q(n')}{g(n')} . \tag{4.9}$$

In the limit $N_{ex} \gg 1$, the behavior of $P(n)$ is dominated by the exponential term in (4.8). As noted earlier, the photon-number distribution then tends to accumulate in the global minimum of the effective potential. The extrema of the effective potential are found by requiring that $\partial V/\partial n=0$, or $q(n)=0$. This reproduces the semiclassical steady-state solutions given by Eq. (4.5). (Note that the semiclassical unstable solutions shown in Fig. 3 correspond to the maxima of the potential.) Figure 5 shows the effective potential as a function of n for three values of Θ in the region of the second maser threshold; see Fig. 1. In each case shown here $V(n)$ exhibits two minima. For $\Theta=5$ the global minimum occurs at $n_1 \cong 0.24$, whereas for $\Theta=7$ it appears at $n_2 \cong 0.6$. At $\Theta=6$ the minima are degenerate. Therefore, just below $\Theta_c=6$, n_1 is the global minimum, whereas, for $\Theta > \Theta_c$, n_2 takes over as the global minimum. The mechanism for the higher-order thresholds is clearly always the same, with a minimum n_m of $V(n)$ losing its global character and being replaced by the next one n_{m+1}. The mth maser

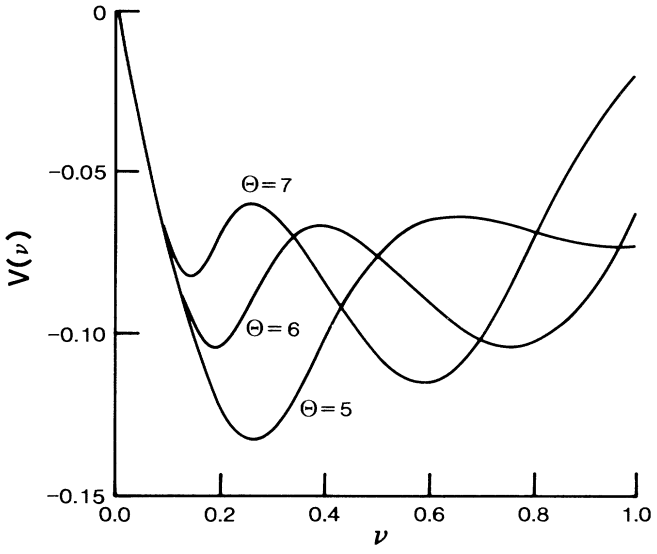

FIG. 5. Effective potential $V(\nu)$ as a function of ν for $\Theta=5,6,7$. The left-hand minimum is the global minimum for $\Theta<6$, whereas for $\Theta>6$ the right-hand-side minimum is the global minimum.

threshold occurs when $P(\nu_{m-1})=P(\nu_m)$. Then, assuming $N_{\rm ex}\gg 1$ so that the exponential term in Eq. (4.8) dominates, we obtain the condition

$$\int_0^{\nu_{m-1}} \frac{d\nu' q(\nu')}{g(\nu')} = \int_0^{\nu_m} \frac{d\nu' q(\nu')}{g(\nu')} , \tag{4.10a}$$

or

$$\int_{\nu_{m-1}}^{\nu_m} \frac{d\nu' q(\nu')}{g(\nu')} = 0 . \tag{4.10b}$$

Equation (4.10b) can be used to find that value of Θ at which the mth threshold occurs. The vertical dotted line in Fig. 4 indicates the transition from the first to the second branch (second maser threshold) as predicted by Eq. (4.10b). This is in good quantitative agreement with the quantum analysis. Similar results are obtained for the higher-order maser thresholds.

These results indicate that we can obtain a reasonable approximation to the full quantum calculations by supplementing the semiclassical steady states given by $q(\nu_m)=0$ by rule (4.10b) to calculate the transition between the various semiclassical branches. Equation (4.10b) always predicts a vertical transition between branches, which also occurs in the quantum calculations in the limit $N_{\rm ex}\to\infty$. This suggests that, in the language of equilibrium thermodynamics, $N_{\rm ex}\to\infty$ is analogous to the thermodynamic limit. The first maser threshold is like a second-order phase transition, whereas the higher-order transitions are like first-order phase transitions. This interpretation is further strengthened by recognizing that V plays the role of a generalized Ginzburg-Landau potential, and that Eq. (4.10a) is an equal-area rule akin to the Maxwell construction. This construction is a consequence of the condition that in homogeneous systems the transition between two phases occurs when their Ginzburg-Landau potentials are equal, $V(\nu_{m-1})=V(\nu_m)$. In the semiclassical theory the various (stable) branches of the steady-state curve are distinguished by the fact that they correspond to different numbers of Rabi oscillations of the atomic Bloch vector as the atoms traverse the cavity. For the mth minimum of the effective potential the Bloch vector undergoes $2m$ complete Rabi oscillations. This feature also serves to identify the different "phases" of the micromaser. In this picture the various minima of the effective potential play the role of the different phases which are possible configurations of the system, and the Ginzburg-Landau potential determines which phase is observed.

C. Two-phase coexistence

In the preceding subsection we considered a theory in which the branches of the semiclassical steady states are connected discontinuously according to the equal-area rule (4.10b). In our thermodynamical analogy the various branches are interpreted as different phases of the system. Our assumption was that for $\tau\to\infty$ only one phase remains for a given Θ. This model may be extended by considering the statistical average

$$\langle\nu\rangle = \frac{1}{Z}\sum_m \nu_m P(\nu_m) , \tag{4.11a}$$

where

$$Z = \sum_m P(\nu_m) \tag{4.11b}$$

is a normalization constant analogous to the partition function. $P(\nu_m)$ is the probability that $\nu=\nu_m$ according to Eq. (4.8), and the index m runs over the minima of the effective potential. A comparison between the exact

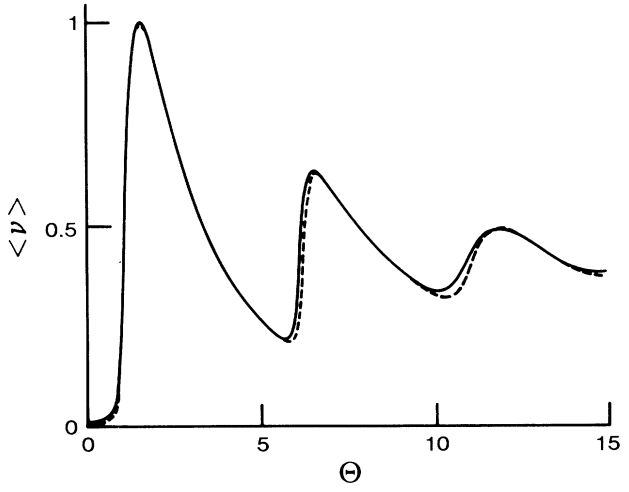

FIG. 6. Comparison of the normalized mean photon number $\langle\nu\rangle$ as calculated using the full quantum theory (solid line) and the statistical average of the semiclassical steady states given by Eqs. (4.11) (dashed line).

quantum calculation and Eq. (4.11) is shown in Fig. 6, and excellent agreement is observed. The new ingredient introduced by the averaging procedure (4.11) is that we now allow for more than one phase to be present for any given value of Θ. In particular, around any one maser threshold the system changes between two phases. Equation (4.11) allows for two-phase coexistence with the appropriate statistical mixture of the two participating phases. This leads to smoothing out of the maser thresholds as is observed in the full quantum calculations.

V. CONCLUSION

In this paper we have presented a consistent semiclassical theory of the micromaser based on a multiple-time-scale analysis. Such an approach presents the considerable advantage of unambiguously isolating the time scales over which semiclassical and (quantum-) fluctuation-dominated dynamics take place. It also explicitly shows that semiclassical and long-time limits do not commute.

We have shown that a reasonable approximation to the full quantum calculations can be achieved by supplementing the semiclassical steady states by an equal-area Maxwell rule to calculate the transition between the various semiclassical branches. This interpretation is based on the observation that the effective potential V describing the micromaser plays the role of a generalized Ginzburg-Landau potential. In this picture the various minima of the effective potential corresponds to the different phases which are possible configurations of the system, and the Ginzburg-Landau potential determines which phase is observed. This paper concentrated on steady-state properties of the micromaser. Future work will show how the multiple-time-scale approach can be used to identify the remnants of classical features such as instabilities and chaos in the approach to the quantum-mechanical steady state.

ACKNOWLEDGMENTS

This work was supported by Office of Naval Research Contract No. N00014-88-K-0294 and by National Science Foundation Grant No. PHY-86-03368. One of us (A.M.G.) was supported in part by the Joint Services Optical Program, and numerical work was performed in part at the John von Neuman Computer Center, Princeton.

---

*Permanent address: Departamento de Fisica, Universidad Nacional de Colombia, Bogota, Columbia.

[1]See, e.g., S. Haroche and D. Kleppner, Phys. Today **42**(1), 24 (1989).

[2]D. Meschede, H. Walther, and G. Mueller, Phys. Rev. Lett. **54**, 551 (1985).

[3]M. Brune, J. M. Raimond, and S. Haroche, Phys. Rev. A **35**, 154 (1987); M. Brune, J. M. Raimond, P. Goy, L. Davidovich, and S. Haroche, Phys. Rev. Lett. **59**, 1899 (1987).

[4]P. Filipowicz, J. Javanainen, and P. Meystre, Phys. Rev. A **34**, 3077 (1986).

[5]L. Davidovich, J. M. Raimond, M. Brune, and S. Haroche, Phys. Rev. A **36**, 3771 (1987).

[6]P. Meystre, G. Rempe, and H. Walther, Opt. Lett. **13**, 1078 (1988).

[7]G. Rempe, H. Walther, and N. Klein, Phys. Rev. Lett. **58**, 353 (1987); E. M. Wright and P. Meystre, Opt. Lett. **14**, 177 (1989).

[8]See, e.g., S. W. Koch, *Dynamics of First-Order Phase Transitions in Equilibrium and Nonequilibrium Systems* (Springer-Verlag, Berlin, 1984).

[9]See, e.g., W. H. Louisell, *Quantum Statistical Properties of Radiation* (Wiley, New York, 1973).

[10]E. T. Jaynes and F. W. Cummings, Proc. IEEE. **51**, 89 (1963).

[11]See, e.g., H. Risken, *The Fokker-Planck Equation, Method of Solution and Applications,* Vol. 18 of *Springer Series in Synergetics,* edited by H. Haken (Springer-Verlag, Berlin, 1984).